PCCP

PAPER

View Article Online
View Journal | View Issue

Cite this: *Phys. Chem. Chem. Phys.*, 2016, **18**, 18128

Optical properties of the hydrated charged silver tetramer and silver hexamer encapsulated inside the sodalite cavity of an LTA-type zeolite†

Ngo Tuan Cuong,*[a] Hue Minh Thi Nguyen,[a] My Phuong Pham-Ho*[b] and Minh Tho Nguyen[c]

Received 2nd April 2016,
Accepted 10th June 2016

DOI: 10.1039/c6cp02037b

www.rsc.org/pccp

The optical spectra in the UV-VIS region of the hydrated doubly charged tetramer Ag_4^{2+} and hydrated multiply charged hexamer Ag_6^{p+} silver clusters encapsulated inside the sodalite cavity of an LTA-type zeolite have been systematically predicted using DFT, TD-DFT and CASSCF/CASPT2 methods. The optical behaviour of the model hydrated clusters $[Ag_6(H_2O)_8(Si_{24}H_{24}O_{36})]^{p+}$ is very sensitive to their charge. Among the cations $[Ag_6(H_2O)_8(Si_{24}H_{24}O_{36})]^{p+}$, only the embedded hydrated quadruply charged silver hexamer $[Ag_6(H_2O)_8(Si_{24}H_{24}O_{36})]^{4+}$ shows a strong absorption band at ~420 nm (blue light) and emits light in red color. The absorption spectrum of the hydrated doubly charged silver tetramer cluster $[Ag_4(H_2O)_m(Si_{24}H_{24}O_{36})]^{2+}$, which shifts slightly and steadily with the increasing amount of interacting water molecules to longer wavelengths, has a strong peak in the blue region. The water environment forces the silver tetramer to relocate into one side of the cavity instead of at its center as in the case of the non-hydrated $[Ag_4(Si_{24}H_{24}O_{36})]^{2+}$ cluster. Water molecules act as ligands significantly splitting the energy levels of excited states of the Ag_4^{2+} and Ag_6^{4+} clusters. This causes the absorption spectra of the clusters to broaden and the emission to shift to the green-yellow and red part of the visible region.

1. Introduction

Investigations on silver clusters have continuously been carried out for decades,[1–29] and recently the charged silver clusters dispersed in media such as oxyfluoride glass and zeolite cavities have been prepared and optically investigated.[30–36] An emerging view is that the silver clusters, which are the associations of silver atoms and ions, present a molecule-like behavior featuring discrete energy levels. When interacting with photons, they undergo electronic transitions and as a result, absorption and emission occur as in any molecular system. Many studies also showed that encapsulation of a charged silver cluster in a restricted environment of a zeolite host is expected to change the guest properties. Through host–guest interactions, even unstable silver clusters could be stabilized to exist inside a nanometer-size cavity of a host.[34,35] Sometimes the inner cations aggregate to form unusually small clusters, due to the stabilizing electrostatic interactions with the negatively charged oxygen atoms of zeolites. For example, small silver clusters consisting of 2–8 atoms have been reported to exist inside zeolite cavities.[34–53] Depending on the sizes and the charges of the enclosed silver species, the embedded zeolites often exhibit unique opto-electronic properties. For instance, the Ag_3^{n+} and Ag_6^{m+} clusters can be formed within Faujasite (FAU) and Linde Type A (LTA) zeolites and become fluorescent after calcination.[51] Recently, the Ag_{14} cluster has experimentally been found to be formed inside a sodalite cavity of an LTA zeolite.[54] The actual charge of the Ag_{14} cluster formed in this zeolite environment, the nature of such association, the metal–metal interactions as well as the role of the sodalite cavity incarcerating silver atoms and ions in its center have been analyzed in a recent theoretical study.[55]

The small positively charged silver clusters, when being encapsulated inside zeolite cavities, could also exist in hydrated forms. For instance, the emission of thermally treated Ag activated zeolite Na-A upon dehydration/hydration in vacuum/water vapor has been observed experimentally.[56] Although the characteristic yellow-green emission has been assigned to be strongly associated with the coordinating water molecules to the Ag^+ ions or Ag^0 atoms,[56] to the best of our knowledge, the effect of interactions between water molecules and silver clusters on the resulting optical properties is not well understood yet. In this context, we set out to carry out in this work a theoretical investigation of the small Ag_4 and Ag_6 charged clusters and their hydrated forms

[a] *Center for Computational Science and Faculty of Chemistry, Hanoi National University of Education, Hanoi, Vietnam. E-mail: cuongnt@hnue.edu.vn*
[b] *Institute for Computational Science and Technology (ICST), Ho Chi Minh City, Vietnam. E-mail: phmphuong@yahoo.com*
[c] *Department of Chemistry, KU Leuven, B-3001 Leuven, Belgium*

† Electronic supplementary information (ESI) available. See DOI: 10.1039/c6cp02037b

encapsulated in the sodalite cavity of an LTA-type zeolite. We are interested in determining how the optical behaviour of the clusters changes with respect to the charge, and the amount of interacting water molecules, as well as the role of the latter.

2. Methods of calculation

We first construct a non-substituted zeolite model including a six-membered ring (6-MR) cavity, a composite building unit, or a sodalite (SOD 24T) cavity. This simplest model has a $Si_{24}O_{36}$ framework whose silicon atoms are all saturated by hydrogen atoms.[55] As a result, the chemical formula of the host is $Si_{24}H_{24}O_{36}$, as shown in Fig. 1. To construct the hydrated and positively charged silver cluster $Ag_n(H_2O)_m^{p+}$ embedded model, we add silver atoms and water molecules inside the cavity of the $Si_{24}H_{24}O_{36}$ framework and then optimize the resulting structures. The chemical formula of the resulting cluster is thus $[Ag_n(H_2O)_mSi_{24}H_{24}O_{36}]^{p+}$. The most plausible configuration of the cluster can then be determined.

Using the method of density functional theory (DFT),[57] we optimize the geometries of the $[Ag_n(H_2O)_mSi_{24}H_{24}O_{36}]^{p+}$ clusters in such a way that the geometry of the surrounding sodalite cage is fixed and the hydrated and charged silver clusters are relaxed converging to energy minima in their ground electronic state. The harmonic vibrational frequency calculations are followed to confirm the optimized stationary points as energy minima (with all real frequencies). In the following stage, time-dependent density functional theory (TD-DFT)[58–62] calculations are performed to identify the electron transitions from the ground to excited states that are responsible for the absorption spectra.

The popular hybrid B3LYP functional[63] is employed in both DFT and TD-DFT calculations. Due to the relatively large size of the systems considered, the Los Alamos National Laboratory 2-Double Zeta (LANL2DZ) basis set[64] is used in conjunction with the B3LYP functional. This basis set combines effective core potential (ECP) basis sets for Al, Si, and Ag and the valence basis sets for O and H atoms. All calculations are performed using the Gaussian09 package.[65] In the last stage of calculations, we use the methods of complete active space second-order perturbation theory based on complete active space self-consistent-field wavefunctions (CASSCF/CASPT2 method), and the restricted active space state interaction (RASSI method) to simulate the emission process of the investigated cluster using the Molcas package.[66–69]

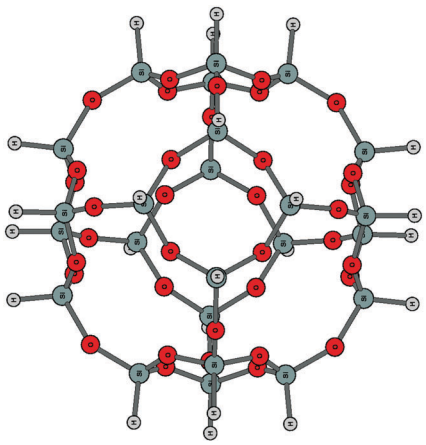

Fig. 1 The structure of the $Si_{24}H_{24}O_{36}$ host. The red circles represent O atoms; the small grey circles represent H atoms and dark-green circles represent Si atoms.

3. Results and discussion

3.1. The $[Ag_6(H_2O)_8(Si_{24}H_{24}O_{36})]^{p+}$ hydrated clusters

We started our investigation of the optical properties of hydrated charged silver clusters embedded in the zeolite cavity from the hydrated charged silver hexamers encapsulated inside the sodalite cavity of an LTA-type zeolite, namely the $[Ag_6(H_2O)_8(Si_{24}H_{24}O_{36})]^{p+}$ clusters. Geometries of these clusters with different charges p = 1, 2,... 6 are optimized at the B3LYP/LANL2DZ level and illustrated in Fig. S1a–e of the ESI† file. The cationic silver clusters are located at the center of the sodalite cavity in which silver atoms/ions point toward the four-membered rings of the cavity (there are six four-membered rings). The eight water molecules are located at the vicinity of the six-membered rings inside the cavity and surround the silver cluster.

TD-DFT calculations are performed on the optimized geometries to evaluate the transition energies from the ground to excited states, and thereby simulate the absorption spectra. The average Ag–Ag bond length, the HOMO–LUMO gap, the NBO charge on Ag_6, transition energies and the first low-spin excited state with respect to different charges p of the whole $[Ag_6(H_2O)_8(Si_{24}H_{24}O_{36})]^{p+}$ are listed in Table 1. As could be seen in Table 1 the average Ag–Ag distance decreases slightly from 2.770 Å in $[Ag_6(H_2O)_8Si_{24}H_{24}O_{36}]^{1+}$ to 2.766 Å in $[Ag_6(H_2O)_8Si_{24}H_{24}O_{36}]^{3+}$ and 2.768 Å in $[Ag_6(H_2O)_8Si_{24}H_{24}O_{36}]^{4+}$ and then increases to 2.862 Å in $[Ag_6(H_2O)_8Si_{24}H_{24}O_{36}]^{5+}$ and 2.990 Å in $[Ag_6(H_2O)_8Si_{24}H_{24}O_{36}]^{6+}$. Transition energies between the ground and low spin excited states as well as the absorption spectra of the clusters are shown in Fig. S2 and S3 in the ESI† file. We also see from Table 1 that amongst the investigated clusters, only $[Ag_6(H_2O)_8(Si_{24}H_{24}O_{36})]^{p+}$ with p = 4, 5, and 6 have transition energies between the ground and first singlet excited states located in the visible region. The other clusters have smaller excitation gaps.

The absorption spectra of the $[Ag_6(H_2O)_8(Si_{24}H_{24}O_{36})]^{p+}$ clusters with p = 4, 5, 6 are plotted in Fig. 2. Accordingly, the absorption spectrum of the $[Ag_6(H_2O)_8(Si_{24}H_{24}O_{36})]^{6+}$ cluster is

Table 1 The average Ag–Ag bond length, the HOMO–LUMO gap, the NBO charge on the Ag_6 cluster and the energy gap between the ground and the first low spin excited state of the $[Ag_6(H_2O)_8(Si_{24}H_{24}O_{36})]^{p+}$ cluster (B3LYP/LANL2DZ)

p	1	2	3	4	5	6
d(Ag–Ag), Å	2.770	2.776	2.766	2.768	2.862	2.990
HOMO–LUMO gap	1.0	1.9	1.7	3.3	3.2	4.2
GS-EX_1 gap, eV	0.39	1.17	0.94	2.87	2.44	3.35
NBO charge on Ag_6	1.2	2.3	1.7	3.4	3.4	4.9

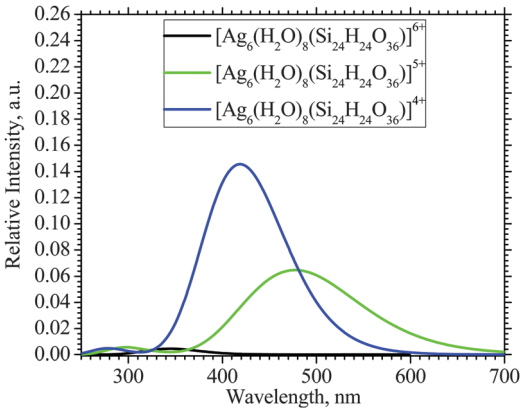

Fig. 2 Absorption spectra of the $[Ag_6(H_2O)_8(Si_{24}H_{24}O_{36})]^{p+}$ clusters. The black curve represents $[Ag_6(H_2O)_8(Si_{24}H_{24}O_{36})]^{6+}$; the green curve represents $[Ag_6(H_2O)_8(Si_{24}H_{24}O_{36})]^{5+}$; and the blue curve represents $[Ag_6(H_2O)_8(Si_{24}H_{24}O_{36})]^{4+}$. The full width at half maximum is 0.333 eV (B3LYP/LANL2DZ). Absorption intensities of the clusters are relative to each other.

characterized by a very weak absorption band in the visible region, as compared to that of the $[Ag_6(H_2O)_8(Si_{24}H_{24}O_{36})]^{4+}$ and the $[Ag_6(H_2O)_8(Si_{24}H_{24}O_{36})]^{5+}$ clusters. The $[Ag_6(H_2O)_8(Si_{24}H_{24}O_{36})]^{4+}$ cluster possesses a singlet ground state with all electrons paired, while the $[Ag_6(H_2O)_8(Si_{24}H_{24}O_{36})]^{5+}$ cluster has a doublet ground state with one unpaired electron. We therefore set out to pursue further investigation on the optical behavior of the $[Ag_6(H_2O)_8(Si_{24}H_{24}O_{36})]^{4+}$ cluster which is a closed-shell diamagnetic system.

The densities of state (DOS) of the $[Ag_6(H_2O)_8(Si_{24}H_{24}O_{36})]^{4+}$ cluster are plotted in Fig. 3. This has in its ground state two electrons in the outer shell. The HOMO's energy of the $[Ag_6(H_2O)_8(Si_{24}H_{24}O_{36})]^{4+}$ cluster is far higher than that of the inner orbitals, as could be seen in Fig. 3. The cluster is in a C_i point group and its ground electronic state corresponds to the ^1A_g: $[\ldots(a_g)^2(a_u)(a_u)(a_u)\ldots]$ orbital configuration in the outer shell. These four frontier orbitals, namely HOMO, LUMO, LUMO+1 and LUMO+2, are constructed mainly from the AO(5s) of silver

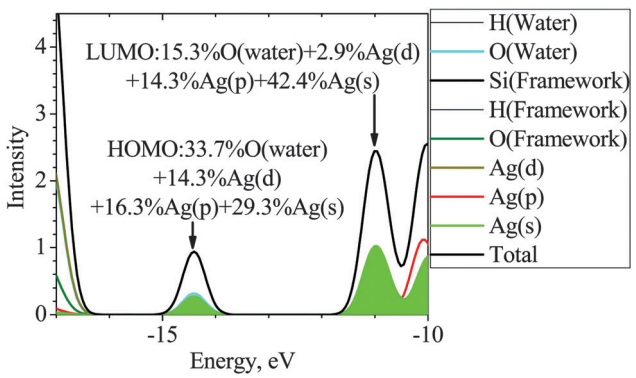

Fig. 3 Densities of state of $[Ag_6(H_2O)_8(Si_{24}H_{24}O_{36})]^{4+}$ (B3LYP/LANL2DZ). The solid black lines denote the total DOS and the s(Ag) component is shown by the shaded green area. The intensity corresponds to the number of MOs. Contributions to the HOMO and LUMO of AOs of oxygen and silver atoms are represented in the inset.

atoms and significantly from orbitals of water molecules. The shapes of these frontier orbitals and their relative energies are presented in Fig. S4 of the ESI† file.

The calculated absorption spectrum of $[Ag_6(H_2O)_8(Si_{24}H_{24}O_{36})]^{4+}$, which is broadened with the full width at half maximum equal to 0.33 eV, has one strong peak centered at ~420 nm. The latter is due to the convolution of the two electronic transitions of which one is from the ground state to the first singlet excited state ($S_0 \rightarrow S_1$) and the other is from the ground state to the second singlet excited state ($S_0 \rightarrow S_2$). In other words, this absorption band arises from electronic transitions from the HOMO to the LUMO and from the HOMO to LUMO+1 as well as LUMO+2 in the region of frontier orbitals.

In order to probe the effect of Al-substitution on the optical properties of the Ag_6^{4+} cluster, we perform calculations on the hydrated-Ag_6^{4+} encapsulated inside an Al-substituted framework, namely the $[Ag_6(H_2O)_8(Al_4Si_{20}H_{24}O_{36})]^0$ cluster. The reason for the choice of such an Al-substituted framework having four Al atoms shall be discussed as follows. The substitution of one Al^{3+} for one Si^{4+} on the SiO_2 framework should induce one-electron negative charge on the framework. Therefore, in the $[Ag_6(H_2O)_8(Al_4Si_{20}H_{24}O_{36})]^0$ cluster the $(Al_4Si_{20}H_{24}O_{36})$ framework has four-electron negative charge and the $Ag_6(H_2O)_8$ cluster has four-electron positive charge. In other words, the chemical formula could be written as $[Ag_6(H_2O)_8{}^{4+}(Al_4Si_{20}H_{24}O_{36})^{4-}]^0$. To confirm this assumption, we analyze the NBO charges of the investigated cluster. The NBO charge on the Ag_6 cluster is +3.4 electron, the average Ag–Ag bond length is 2.76 Å and the HOMO–LUMO gap is 3.4 eV. The absorption spectrum of $[Ag_6(H_2O)_8(Al_4Si_{20}H_{24}O_{36})]^0$, which is plotted in Fig. 4, has one strong absorption band centered at 425 nm due again to the convolutions of both $S_0 \rightarrow S_1$ and $S_0 \rightarrow S_2$ electronic transitions. These properties are the same as compared to the case of the $[Ag_6(H_2O)_8(Si_{24}H_{24}O_{36})]^{4+}$ cluster.

It has also been demonstrated that instead of modeling the absorption spectra of the non-hydrated silver clusters embedded inside the Al-substituted sodalite cavity of an LTA-type zeolite as it is usual in reality, we can simulate the absorption spectra of these silver clusters encapsulated inside the non-substituted sodalite cavity, which is less complicated, with an appropriate formal charge on the whole model.[55]

In this research work attempt is made to do an in-depth study of the effect of hydrated-water molecules on absorption properties of the encapsulated charged silver clusters. To clarify this crucial importance, we investigate in this Section, together with the Ag_4^{2+} in the later section, the embedded non-hydrated charged silver cluster Ag_6^{4+}, namely the $[Ag_6(Si_{24}H_{24}O_{36})]^{4+}$ cluster as well as some low-hydrated $[Ag_6(H_2O)_4(Na_4Al_8Si_{16}H_{24}O_{36})]^0$ $[Ag_6(H_2O)_5(Na_3Al_7Si_{17}H_{24}O_{36})]^0$ and $[Ag_6(H_2O)_6(Na_2Al_6Si_{18}H_{24}O_{36})]^0$ clusters. Of the latter clusters, the cage framework now contains some levels of Al-substitution and the Na atoms as well as the water molecules are in the vicinities of six-membered rings. We thus optimize the structures and perform TD-DFT calculations on the optimized geometries of the clusters. Both optimized structures of the $[Ag_6(Si_{24}H_{24}O_{36})]^{4+}$ and the $[Ag_6(H_2O)_8(Si_{24}H_{24}O_{36})]^{4+}$ clusters are presented in Fig. 5. Absorption spectra of the low-hydrated

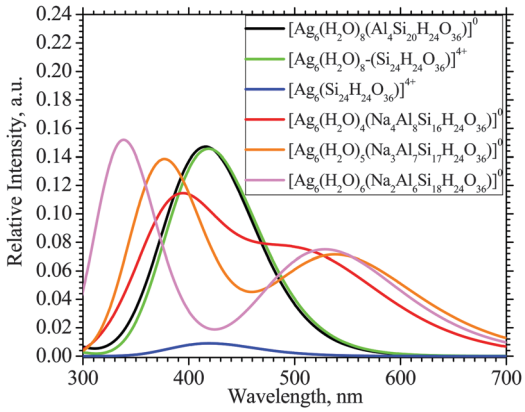

Fig. 4 Absorption spectra of the $[Ag_6(Si_{24}H_{24}O_{36})]^{4+}$, $[Ag_6(H_2O)_8(Si_{24}H_{24}O_{36})]^{4+}$, $[Ag_6(H_2O)_8(Al_4Si_{20}H_{24}O_{36})]^0$, $[Ag_6(H_2O)_4(Na_4Al_8Si_{16}H_{24}O_{36})]^0$ and $[Ag_6(H_2O)_5(Na_3Al_7Si_{17}H_{24}O_{36})]^0$ clusters. The black curve represents $[Ag_6(Si_{24}H_{24}O_{36})]^{4+}$; the green curve represents $[Ag_6(H_2O)_8(Si_{24}H_{24}O_{36})]^{4+}$; and the blue curve represents $[Ag_6(H_2O)_8(Al_4Si_{20}H_{24}O_{36})]^0$; the red curve represents $[Ag_6(H_2O)_4(Na_4Al_8Si_{16}H_{24}O_{36})]^0$; the orange curve represents $[Ag_6(H_2O)_5(Na_3Al_7Si_{17}H_{24}O_{36})]^0$. The full width at half maximum is 0.333 eV (TD-DFT with B3LYP/LANL2DZ).

$[Ag_6(H_2O)_4(Na_4Al_8Si_{16}H_{24}O_{36})]^0$, $[Ag_6(H_2O)_5(Na_3Al_7Si_{17}H_{24}O_{36})]^0$ and $[Ag_6(H_2O)_6(Na_2Al_6Si_{18}H_{24}O_{36})]^0$ clusters which are integrated in Fig. 4 in comparison with that of non-hydrated and fully hydrated Ag_6^{4+} clusters have two obvious absorption bands of which one is at 530 nm and the others are at 390, 380 and 345 nm, respectively. That is due to the distorted geometry of the Ag_6 cluster caused by the direct interactions of silver atoms/ions with the framework where no water molecules are present. The Cartesian coordinates of these clusters are represented in the ESI† file.

Geometrical parameters such as the nearest Ag–O, Ag–Ag contact distances and the coordination numbers are listed in Table 2. Transition energies between the ground and the lowest-lying singlet excited state are schematically illustrated in Fig. 6, in comparison with the hydrated $[Ag_6(H_2O)_8(Si_{24}H_{24}O_{36})]^{4+}$ cluster.

The lowest-lying singlet and triplet excited states of $[Ag_6(Si_{24}H_{24}O_{36})]^{4+}$ are of three-fold degeneracy. The LUMO, LUMO+1 and LUMO+2 of $[Ag_6(Si_{24}H_{24}O_{36})]^{4+}$ are in a T representation of the O_h point group and atomic p-like orbitals. The result shows that the hydrated-water molecules form a ligand field interacting with and splitting the excited states of the encapsulated Ag_6^{4+} moiety. It is noteworthy that the quadruply charged hexamer Ag_6^{4+} is not a stable association itself in the gaseous state, even when it is surrounded by eight water molecules. It is stabilized when being encapsulated inside and electrostatically interacting with the sodalite cavity. The role of water molecules in this case is not to stabilize the association of six silver atoms and ions but to perturb and to split the excited states, and thereby to increase absorption intensity of the encapsulated Ag_6^{4+} cluster.

The results presented in Fig. 6 indicate that the water environment actually splits the singlet and triplet excited states so that the emission occurring from the lowest triplet state, as compared to the absorption, will shift very much to the longer wavelength in the visible region.

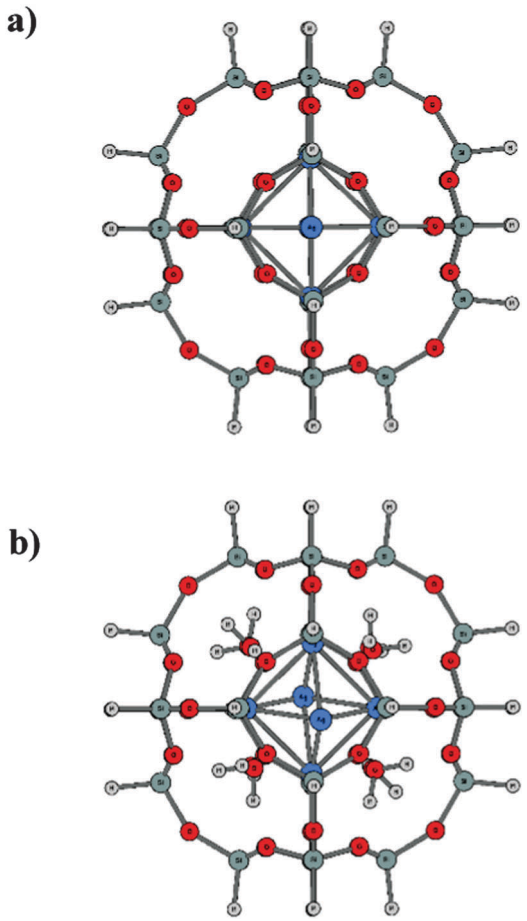

Fig. 5 Optimized geometries of the $[Ag_6(Si_{24}H_{24}O_{36})]^{4+}$ and $[Ag_6(H_2O)_8(Si_{24}H_{24}O_{36})]^{4+}$ clusters. Silver atoms are in blue color. (a) The $[Ag_6(Si_{24}H_{24}O_{36})]^{4+}$ cluster; the average Ag–Ag bond distance is 2.958 Å. (b) The $[Ag_6(H_2O)_8(Si_{24}H_{24}O_{36})]^{4+}$ cluster; the average Ag–Ag bond distance is 2.768 Å (B3LYP/LANL2DZ).

3.2. The $[Ag_4(H_2O)_m(Si_{24}H_{24}O_{36})]^{2+}$ hydrated clusters

Prior to the investigation of the $[Ag_4(H_2O)_m(Si_{24}H_{24}O_{36})]^{2+}$ clusters, we perform calculations on the Ag_4^{2+} cluster in the gas phase and the Ag_4^{2+} cluster encapsulated inside the sodalite cavity of an LTA-type zeolite, giving the $[Ag_4(Si_{24}H_{24}O_{36})]^{2+}$ model. The most stable gas phase structure of Ag_4^{2+} is in the T_d point group with the orbital configuration in the outer shell being $[\ldots(a_1)^2(t_2)^0(t_2)^0(t_2)^0\ldots]$.

The transition energy gap between the ground and lowest-lying singlet excited state is calculated at 4.6 eV (B3LYP/LANL2DZ). When the Ag_4^{2+} cluster is encapsulated inside the framework, this gap becomes smaller amounting to 4.2 eV. The $[Ag_4(Si_{24}H_{24}O_{36})]^{2+}$cluster is also in a proper tetrahedral shape (T_d symmetry) with each of the silver atoms pointing toward six-membered rings of the cavity. The average Ag–Ag bond length is 2.94 Å, which is slightly longer than the Ag–Ag bond length in the gas phase Ag_4^{2+} cluster, being 2.91 Å obtained at the same level. NBO charge of the embedded Ag_4 cluster is approximately +2.0 electron.

The lowest-lying singlet excited states of the $[Ag_4(Si_{24}H_{24}O_{36})]^{2+}$ cluster is also three-fold degenerate, being in T representation in the T_d point group. The calculated absorption spectrum

Table 2 Structural parameters of the $[Ag_6(Si_{24}H_{24}O_{36})]^{4+}$, the $[Ag_6(H_2O)_8(Si_{24}H_{24}O_{36})]^{4+}$ and $[Ag_4(H_2O)_6(Si_{24}H_{24}O_{36})]^{2+}$ cluster (r: contact distance, N: coordination number) (B3LYP/LANL2DZ)

	Short Ag–O		Long Ag–O		Ag–Ag	
Cluster	r/Å	N	r/Å	N	r/Å	N
$[Ag_6(Si_{24}H_{24}O_{36})]^{4+}$	—	—	2.82	4.0	2.96	4.0
$[Ag_6(H_2O)_8(Si_{24}H_{24}O_{36})]^{4+}$	2.35 ± 0.06	2.0	2.78 ± 0.09	4.0	2.77 ± 0.02	4.0
$[Ag_4(H_2O)_6(Si_{24}H_{24}O_{36})]^{2+}$	2.33 ± 0.09	2.5	3.10 ± 0.07	4.0	2.68 ± 0.02	2.5

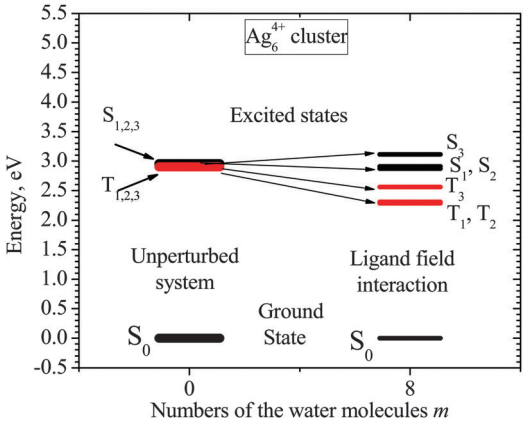

Fig. 6 Splitting diagram for the lowest singlet and triplet excited states of the encapsulated Ag_6^{4+} cluster due to the ligand field formed by water surrounding. Horizontal bars on the left side represent the ground and excited states of the $[Ag_6(Si_{24}H_{24}O_{36})]^{4+}$ cluster; on the right side represent that of the $[Ag_6(H_2O)_8(Si_{24}H_{24}O_{36})]^{4+}$ cluster. Black lines represent the singlet states and red lines represent the triplet state (B3LYP/LANL2DZ).

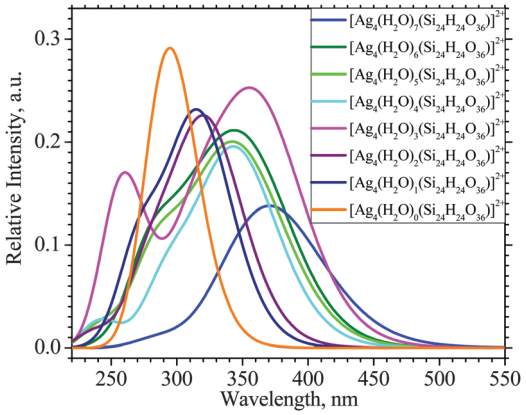

Fig. 7 Calculated absorption spectrum of $[Ag_4(H_2O)_m(Si_{24}H_{24}O_{36})]^{2+}$ clusters with m = 0, 1, 2,. . ., 7 using TD-DFT at B3LYP/LANL2DZ.

$[Ag_4(Si_{24}H_{24}O_{36})]^{2+}$ is illustrated in Fig. 7, in comparison with the embedded hydrated doubly charged tetramer Ag_4^{2+}. The absorption spectrum of the $[Ag_4(Si_{24}H_{24}O_{36})]^{2+}$ cluster has only one strong absorption peak at 295 nm, which is at a longer wavelength as compared to the Ag_4^{2+} cluster in the gas phase, being 267 nm at the same level of calculations.

We now analyze the hydrated doubly charged tetramer $[Ag_4(H_2O)_m(Si_{24}H_{24}O_{36})]^{2+}$, aiming at the role of the interacting water on their optical properties. The numbers of water molecules ranges from m = 1 to 7, being the maximum number of water molecules that could be inside the sodalite cavity.

The structures of $[Ag_4(H_2O)_m(Si_{24}H_{24}O_{36})]^{2+}$ are constructed as follows: from the $[Ag_4(Si_{24}H_{24}O_{36})]^{2+}$ optimized structure, water molecules are added inside the cavity in the vicinity of six-membered rings. The oxygen atom points toward the edges or the faces of the silver clusters whereas the hydrogen atoms point toward the rings. The structures of the resulting $[Ag_4(H_2O)_m(Si_{24}H_{24}O_{36})]^{2+}$ species are optimized and followed by vibrational frequency calculations. TD-DFT calculations using the B3LYP/LAN2DZ method are performed at optimized structures to simulate their absorption spectra.

Several isomers for each m-value of the $[Ag_4(H_2O)_m(Si_{24}H_{24}O_{36})]^{2+}$ clusters are found. The most stable isomers and their relative energies are presented in Fig. S5 and S6 in the ESI† file. TD-DFT calculations using the B3LYP/LAN2DZ functional/basis set are carried out at optimized geometries of all stable isomers in order to evaluate the transition energies from the ground to excited electronic states, and thereby the absorption spectra. The calculated absorption spectra of different isomers of $[Ag_4(H_2O)_m(Si_{24}H_{24}O_{36})]^{2+}$are plotted in Fig. S7 (ESI†). The result shows that the absorption spectra of $[Ag_4(H_2O)_m(Si_{24}H_{24}O_{36})]^{2+}$ isomers differ very much from each other when varying the m-value.

The calculated absorption spectra of the most stable isomers of the $[Ag_4(H_2O)_m(Si_{24}H_{24}O_{36})]^{2+}$ clusters for each value of m = 0, 1, . . ., 7 are plotted in Fig. 7. Exception is found for m = 1 and m = 4 in which the absorption spectra do not correspond to the most stable isomers but rather to the isomers lying at 0.45 and 0.25 eV higher than the ground states, respectively. The reason for such exception is that the absorptions of the most stable isomers of the $[Ag_4(H_2O)_1(Si_{24}H_{24}O_{36})]^{2+}$ and $[Ag_4(H_2O)_4(Si_{24}H_{24}O_{36})]^{2+}$ clusters, which contain nearly planar Ag_4 tetramers, have two and even three separate absorption bands and are not compatible with those of other forms. The excitation energies from the ground to excited states of these $[Ag_4(H_2O)_m(Si_{24}H_{24}O_{36})]^{2+}$ are shown in Fig. 8 as well as Fig. S8 in the ESI† file. Geometrical shapes of the most stable $[Ag_4(H_2O)_m(Si_{24}H_{24}O_{36})]^{2+}$ isomers are shown in Fig. 9.

As could be seen from the plots in Fig. 7 and the energy diagram in Fig. 8, the calculated spectra of the $[Ag_4(H_2O)_m(Si_{24}H_{24}O_{36})]^{2+}$ clusters display one strong absorption band and one vice-peak in the visible region. The energy gap between the ground and the first singlet excited state decreases and the positions of the absorption peaks shift to longer wavelengths when the number of water molecules m increases.

For the non-hydrated $[Ag_4(Si_{24}H_{24}O_{36})]^{2+}$, the calculated absorption band shows only one single peak centered at ~295 nm.

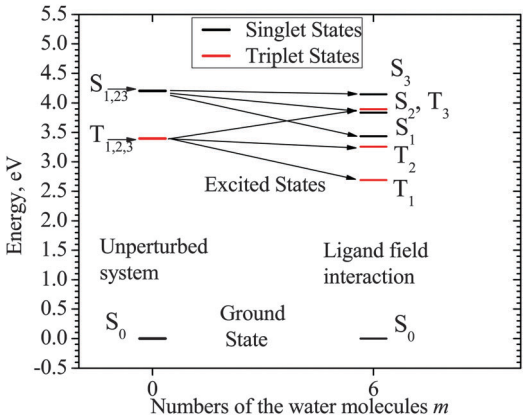

Fig. 8 Splitting diagram for the lowest-lying singlet and triplet excited states of the encapsulated Ag_4^{2+} cluster due to the ligand field formed by water and framework surrounding.

For the hydrated doubly charged tetramers $[Ag_4(H_2O)_m(Si_{24}H_{24}O_{36})]^{2+}$, the calculated absorption spectra show a vice-peak. That is due to the fact that the symmetry of the Ag_4 tetramer is lowered from T_d once the cluster is hydrated resulting in the splitting of the LUMOs, which are three-fold degenerate (in T representative of the T_d point group, or atomic p-like orbitals) for $[Ag_4(Si_{24}H_{24}O_{36})]^{2+}$, and therefore the splitting of the absorption spectra. Such an effect of water molecules on the splitting of energies levels of excited states is represented in Fig. 8, which is quite similar to the case described in Section 3.1 above. In general, the lowest-lying singlet excited state of the embedded Ag_4^{2+} cluster is split once the cluster is hydrated.

The relative intensity of the absorption spectra of $[Ag_4(H_2O)_m(Si_{24}H_{24}O_{36})]^{2+}$ shows that the water surrounding does not affect significantly the intensity of the absorption of the Ag_4^{2+}cluster. The calculated absorption spectra of $[Ag_4(H_2O)_4(Si_{24}H_{24}O_{36})]^{2+}$, $[Ag_4(H_2O)_5(Si_{24}H_{24}O_{36})]^{2+}$ and $[Ag_4(H_2O)_6(Si_{24}H_{24}O_{36})]^{2+}$ which are plotted in Fig. 7, are indeed very similar to each other. In other words, the absorption spectra of the hydrated doubly charged silver tetramer $[Ag_4(H_2O)_m(Si_{24}H_{24}O_{36})]^{2+}$ no longer significantly change when the number of hydrated water molecules reaches the value $m = 4$.

Recently, structural parameters of silver clusters in nanoporous matrices have been investigated using X-ray absorption fine structure (EXAFS) measurements. There is a wide agreement that a nuclearity of four silver atoms/ions in the sodalite cages of heat-treated silver exchanged LTA zeolite is preferred.[34–36] The absorption and emission spectra of the silver clusters have also experimentally been studied revealing that the green/yellow emission was observed in hydrated silver clusters encapsulated inside the sodalite cages of the LTA zeolite.[34–36,56] For the purpose of a subsequent comparison between our theoretical predictions and experimental results, we now analyze the optical properties of $[Ag_4(H_2O)_6(Si_{24}H_{24}O_{36})]^{2+}$ which includes the Ag_4 tetramer in some detail.

The optimized geometry of the most stable isomer of the $[Ag_4(H_2O)_6(Si_{24}H_{24}O_{36})]^{2+}$cluster is presented in Fig. 9 in which the tetramer Ag_4 is in butterfly shape (close to the C_{2v} point group).

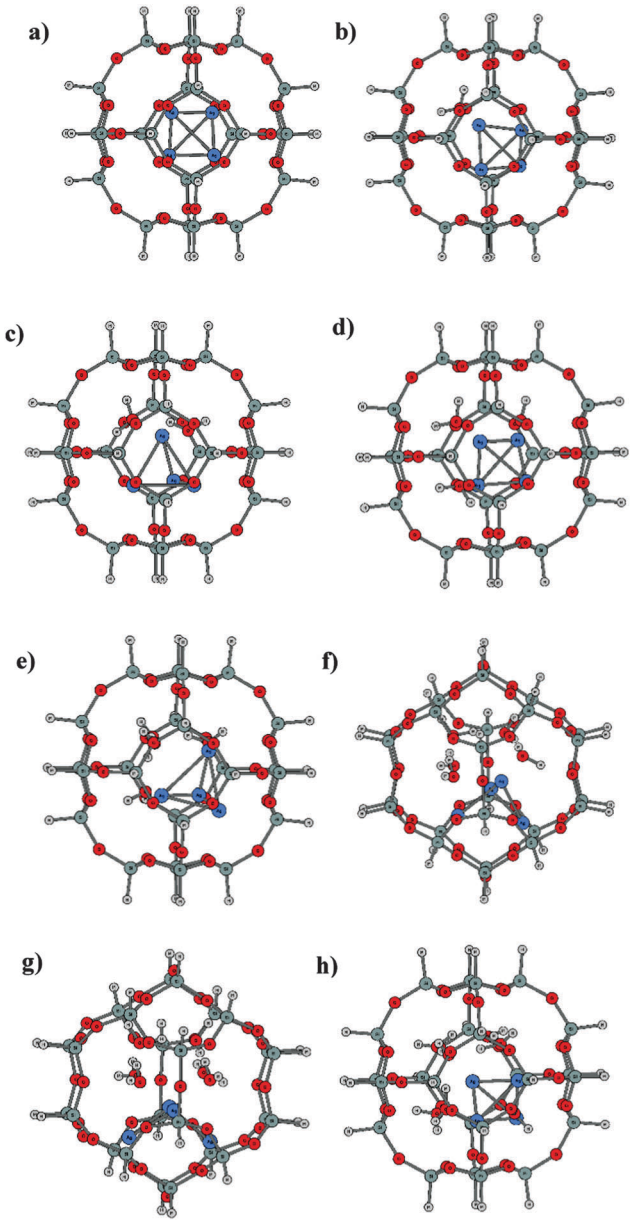

Fig. 9 Structures of $[Ag_4(H_2O)_m(Si_{24}H_{24}O_{36})]^{2+}$ clusters optimized at B3LYP/LANL2DZ. (a) $[Ag_4(Si_{24}H_{24}O_{36})]^{2+}$ cluster; (b) $[Ag_4(H_2O)_1(Si_{24}H_{24}O_{36})]^{2+}$ cluster – isomer1; (c) $[Ag_4(H_2O)_2(Si_{24}H_{24}O_{36})]^{2+}$ cluster – isomer2; (d) $[Ag_4(H_2O)_3(Si_{24}H_{24}O_{36})]^{2+}$ cluster – isomer2; (e) $[Ag_4(H_2O)_4(Si_{24}H_{24}O_{36})]^{2+}$ cluster – isomer3; (f) $[Ag_4(H_2O)_5(Si_{24}H_{24}O_{36})]^{2+}$ cluster – isomer2; (g) $[Ag_4(H_2O)_6(Si_{24}H_{24}O_{36})]^{2+}$ cluster – isomer1; (h) $[Ag_4(H_2O)_7(Si_{24}H_{24}O_{36})]^{2+}$ cluster – isomer1.

The results in Fig. 9g again suggest that water molecules are actually the cause for changes in the position and geometry of the silver tetramer inside the cavity, in going from the center in the case of the $[Ag_4(Si_{24}H_{24}O_{36})]^{2+}$ cluster to the one side of the cavity in the case of the hydrated cluster $[Ag_4(H_2O)_6(Si_{24}H_{24}O_{36})]^{2+}$.

The selected structural parameters such as the nearest Ag–O, the Ag–Ag contact distances and the coordination numbers are listed in Table 2. The six water molecules are located at the centers of six-membered rings on one side of the sodalite cavity, while the silver tetramer is found at the other side.

Of twelve H atoms of the six water molecules, six are towards centres of the rings and six are in between water–O atoms. As could be seen in Fig. S9 of the ESI† file, there are five O–H···O local interactions among the six water molecules in which the average length of the H···O interactions is 1.581 Å, of the O···O distance is 2.566 Å and of the O–H bonds is 1.006 Å – lengthened by 0.030 Å as compared with that of the other O–H bonds in these water molecules. This evidence suggests that the interactions are hydrogen bonds[70] and contribute to the stability of the resulting structure.

Of the four silver atoms, two are located close to the two six-membered rings nearby, and two others bound to two water molecules. The former silver atoms have more positive charge than the latter. On average, each silver atom is surrounded by ~2.5 nearest oxygen atoms including oxygen atoms in water and in the framework with an Ag–O distance of ~2.33 Å. The average Ag–Ag bond length is 2.68 Å and the average coordination number of each silver atom is 2.5 Å.

TD-DFT calculations are performed on the optimized geometry of $[Ag_4(H_2O)_6(Si_{24}H_{24}O_{36})]^{2+}$. Several low-lying singlet and triplet excited states can be identified. Transition energies are presented in Fig. 8 in comparison with those of $[Ag_4(Si_{24}H_{24}O_{36})]^{2+}$. Excited states are split in the case of the hydrated $[Ag_4(H_2O)_6(Si_{24}H_{24}O_{36})]^{2+}$ cluster as compared to the unhydrated $[Ag_4(Si_{24}H_{24}O_{36})]^{2+}$cluster, resulting in a broadening and shifting of the absorption and emission bands to the longer wavelength in the visible region. The lowest triplet and singlet excited states are close and even cross over to each other. As the result, the emission occurring from the lowest triplet state is quenched very much to the longer wavelength in the visible region.

The calculated absorption spectrum of $[Ag_4(H_2O)_6(Si_{24}H_{24}O_{36})]^{2+}$ exhibits one band at ~350 nm and a vice-peak at ~285 nm, as could be seen in Fig. 10. As in the previous case, the main absorption band centered at 350 nm is a convolution of the two electronic transitions from the ground state S_0 to the first and the second singlet excited states S_1 and S_2. The vice-peak is apparently due to an electronic transition from the ground state to higher singlet excited states.

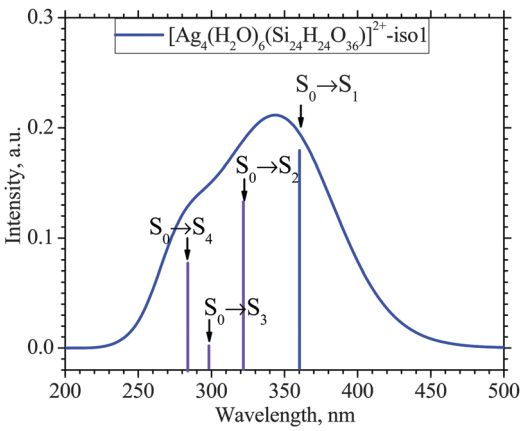

Fig. 10 Simulated absorption spectrum of $[Ag_4(H_2O)_6(Si_{24}H_{24}O_{36})]^{2+}$. The vertical lines represent the electronic transitions from the ground state S_0 to lowest singlet excited states (TD-DFT/B3LYP/LANL2DZ).

3.3. Luminescence of the $[Ag_4(H_2O)_6(Si_{24}H_{24}O_{36})]^{2+}$ cluster

In order to probe further the emission behaviour of the $[Ag_4(H_2O)_6(Si_{24}H_{24}O_{36})]^{2+}$ cluster, we perform two types of calculations. In the first type, the TD-DFT method is used to calculate the single point energy of the ground state (S_0) and excited states including the first (lowest) triplet one (T_1). The energy gap between both triplet state T_1 and ground singlet S_0 states is illustrated in Fig. 11a. In the second type, we carry out CASPT2/CASSCF calculations on a fragment of the optimized structure of the $[Ag_4(H_2O)_6(Si_{24}H_{24}O_{36})]^{2+}$ cluster (given in Fig. 11b). The fragment used for CASPT2/CASSCF calculations includes four silver atoms, four nearest water molecules and six other water molecules corresponding to six oxygen atoms in the framework nearest to the two silver atoms close to the six-membered rings. Such a model used for the CASPT2/CASSCF calculation is the species $[Ag_4(H_2O)_{10}]^{2+}$ for which the structure is illustrated in Fig. 12. The active space selected in this case is a distribution of two electrons amongst four MOs including the HOMO, LUMO, LUMO+1 and LUMO+2. The shapes of the MOs in the active space are illustrated in Fig. S10 in the ESI† file.

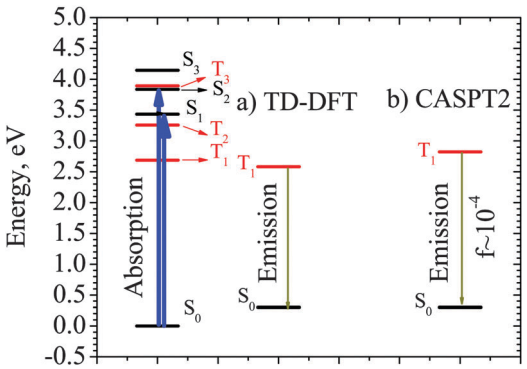

Fig. 11 Transition energies between the lowest triplet T_1 and ground singlet S_0 states at the T_1 state geometry, which is obtained by (a) TD-DFT and (b) CASPT2/CASSCF calculation. The oscillator strength for the $T_1 \rightarrow S_0$ electronic transition calculated by the RASSI calculation is $f \sim 10^{-4}$.

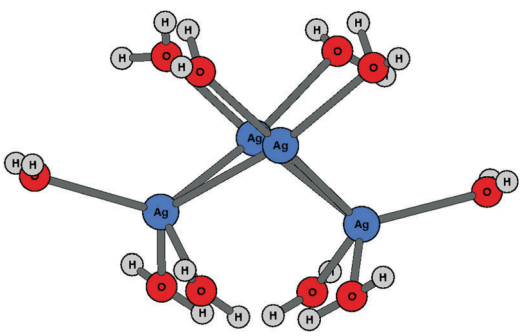

Fig. 12 B3LYP/LANL2DZ structures of $[Ag_4(H_2O)_6]^{2+}$ used for CASPT2 calculations. $[Ag_4(H_2O)_6]^{2+}$ includes six water molecules corresponding to the nearest oxygen atoms of the framework of the sodalite cavity (with Ag–O bond distances approximately equal to 2.4 Å) and four nearest amongst six water molecules in the $[Ag_4(H_2O)_6(Si_{24}H_{24}O_{36})]^{2+}$ cluster (with Ag–O bond distances approximately equal to 2.2 Å).

Transition energy between the triplet excited T_1 and ground singlet S_0 states of the $[Ag_4(H_2O)_6]^{2+}$ model, which is obtained by CASPT2/CASSCF calculations, and the oscillator strength for the $T_1 \rightarrow S_0$ emission obtained by the RASSI calculations including the spin–orbit interaction are presented in Fig. 11b, along with the result of TD-DFT calculations for the purpose of comparison.

Fig. 11 points out that when the $[Ag_4(H_2O)_6(Si_{24}H_{24}O_{36})]^{2+}$ cluster absorbs light at $\sim$350 nm wavelength (the blue absorption), its lowest-lying singlet excited states S_1 and S_2 will be populated. These states are expected to rapidly lose some of the excited state energy and decay to the lowest-lying triplet excited state T_1 by non-radiative processes, such as vibrational relaxation, due to the intermediate states, and the small energy gaps between them.

The luminescence is expected to occur from the lowest-lying triplet excited state T_1, which is located at $\sim$2.27 eV ($\sim$540 nm) according to the TD-DFT calculation, or at $\sim$2.52 eV ($\sim$500 nm) from CASPT2/CASSCF calculations, above the ground state, to the ground state in a long time scale. In other words, for the hydrated doubly charged tetramer encapsulated inside the sodalite cavity of the LTA-type zeolite – $[Ag_4(H_2O)_6(Si_{24}H_{24}O_{36})]^{2+}$ modeled cluster, the absorption is predicted to occur in blue color and the emission in green-yellow color.

4. Concluding remarks

A number of important results emerge from the present theoretical study of some hydrated and charged silver clusters embedded in the cavity of the LTA zeolite. The hydrated doubly charged tetramer Ag_4^{2+} and hydrated multiply charged hexamer Ag_6^{p+} silver clusters encapsulated inside the sodalite cavity of an LTA-type zeolite have been investigated systematically by using DFT, TD-DFT and CASSCF/CASPT2 methods. Their absorption spectra have been simulated theoretically using the TD-DFT method.

The optical behavior of the hydrated model clusters $[Ag_6(H_2O)_8(Si_{24}H_{24}O_{36})]^{p+}$ is changed very much with respect to the charge of the clusters. Of the $[Ag_6(H_2O)_8(Si_{24}H_{24}O_{36})]^{p+}$ clusters considered, only the embedded hydrated quadruply charged silver hexamer $[Ag_6(H_2O)_8(Si_{24}H_{24}O_{36})]^{4+}$ shows a strong absorption band at $\sim$420 nm (blue light) and emits light in red color.

The absorption spectra of the hydrated doubly charged silver tetramer model $[Ag_4(H_2O)_m(Si_{24}H_{24}O_{36})]^{2+}$ change slightly and steadily with the increasing amount of interacting water molecules to longer wavelengths. The water environment forces the silver tetramer to relocate into one side of the cavity instead of at its centre as in the case of the non-hydrated $[Ag_4(Si_{24}H_{24}O_{36})]^{2+}$ cluster. They act as ligands binding to silver ions and atoms. The effect of the generated ligand field of water molecules on the energy levels of excited states of the clusters, and therefore their optical properties, is rather peculiar. This actually splits the excited states of the doubly charged tetramer Ag_4^{2+} and quadruply charged hexamer Ag_6^{4+}, leading to broadening of the absorption spectra in the blue part of the visible region and shifting of the emission to the green-yellow and red part of the visible region.

Acknowledgements

MPPH thanks the Department of Science and Technology of Ho Chi Minh City, Vietnam, for supporting our work at ICST.

References

1 J. Ruamps, *Compt. Rend.*, 1954, **238**, 1489.
2 P. J. Ruamps, *Ann. Phys.*, 1959, **4**, 1111.
3 R. C. Maheshwari, *Indian J. Phys.*, 1963, **37**, 368.
4 H. Handschuh, C. Y. Cha, P. S. Bechthold, G. Gantefor and W. Eberhardt, *J. Chem. Phys.*, 1995, **102**, 6406.
5 V. Beutel, H.-G. Kramer, G. L. Bhale, M. Kuhn, K. Weyers and W. Demtroder, *J. Chem. Phys.*, 1993, **98**, 2699.
6 C. Jackschath, I. Rabin and W. Schulze, *Z. Phys. D*, 1992, **22**, 517.
7 C. Shin-Piaw, W. Loong-Seng and L. Yoke-Seng, *Nature*, 1966, **209**, 1300.
8 T. Diederich, J. Tiggesbaumker and K.-H. Meiwes-Broer, *J. Chem. Phys.*, 2002, **116**, 3263.
9 V. Bonacic-Koutecky, *Angew. Chem., Int. Ed.*, 2011, **50**, 878.
10 V. Bonačić-Koutecký, J. Pittner, M. Boiron and P. Fantucci, *J. Chem. Phys.*, 1999, **110**, 3876.
11 V. Bonačić-Koutecký, J. Burda, R. Mitrić, M. Ge, G. Zampella and P. Fantucci, *J. Chem. Phys.*, 2002, **117**, 3120.
12 V. Bonačić-Koutecký, V. Veyret and R. Mitrić, *J. Chem. Phys.*, 2001, **115**, 10450.
13 H. Deutsch, J. Pittner, V. Bonačić-Koutecký, K. Becker, S. Matt and T. D. Märk, *J. Chem. Phys.*, 1999, **111**, 1964.
14 S. Lecoultre, A. Rydlo and C. Félix, *J. Chem. Phys.*, 2007, **126**, 204507.
15 M. Harb, F. Rabilloud, D. Simon, A. Rydlo, S. Lecoultre, F. Conus, V. Rodrigues and C. Félix, *J. Chem. Phys.*, 2008, **129**, 194108.
16 J. C. Idrobo, S. Ogut and J. Jellinek, *Phys. Rev. B: Condens. Matter Mater. Phys.*, 2005, **72**, 085445.
17 G. F. Zhao, Y. Lei and Z. Zeng, *Chem. Phys.*, 2006, **327**, 261.
18 V. A. Spasov, T. H. Lee, J. P. Maberry and K. M. Ervin, *J. Chem. Phys.*, 1999, **110**, 5208.
19 D. W. Liao and K. Balasubramanian, *J. Chem. Phys.*, 1992, **97**, 2548.
20 S. Liu, Y. Li, X. Zhao, X. Liu and M. Chen, *Spectrochim. Acta, Part A*, 2011, **82**, 205.
21 S. Zhao, Z.-H. Li, W.-N. Wang, Z.-P. Liu, K.-N. Fan, Y. Xie and H. Schaefer, *J. Chem. Phys.*, 2006, **124**, 184102.
22 R. Fournier, *J. Chem. Phys.*, 2001, **115**, 2165.
23 K. A. Bosnick, T. L. Haslett, S. Fedrigo, M. Moskovits, W.-T. Chan and R. Fournier, *J. Chem. Phys.*, 1999, **111**, 8867.
24 E. Janssens, X. J. Hou, M. T. Nguyen and P. Lievens, *J. Chem. Phys.*, 2006, **124**, 184319.
25 Y. Shi, V. A. Spasov and K. M. Ervin, *J. Chem. Phys.*, 1999, **111**, 938.

26 M. Yang, K. A. Jackson and J. Jellinek, *J. Chem. Phys.*, 2006, **125**, 144308.
27 D. W. Silverstein and L. Jensen, *J. Chem. Phys.*, 2010, **132**, 194302.
28 S. Lecoultre, A. Rydlo, J. Buttet, C. Félix, S. Gilb and W. Harbich, *J. Chem. Phys.*, 2011, **134**, 184504.
29 C. Félix, C. Sieber, W. Harbich, J. Buttet, I. Rabin, W. Schulze and G. Ertl, *Chem. Phys. Lett.*, 1999, **313**, 105.
30 N. T. Cuong, V. K. Tikhomirov, L. F. Chibotaru, A. Stesmans, V. D. Rodríguez, M. T. Nguyen and V. V. Moshchalkov, *J. Chem. Phys.*, 2012, **136**, 174108.
31 J. J. Velázquez, V. K. Tikhomirov, L. F. Chibotaru, N. T. Cuong, A. S. Kuznetsov, V. D. Rodríguez, M. T. Nguyen and V. V. Moshchalkov, *Opt. Express*, 2012, **20**, 13582.
32 A. S. Kuznetsov, N. T. Cuong, V. K. Tikhomirov, M. Jivanescu, A. Stesmans, L. F. Chibotaru, J. J. Velázquez, V. D. Rodríguez, D. Kirilenko, G. Van Tendeloo and V. V. Moshchalkov, *Opt. Mater.*, 2012, **34**, 616.
33 M. V. Shestakov, N. T. Cuong, V. K. Tikhomirov, M. T. Nguyen, L. F. Chibotaru and V. V. Moshchalkov, *J. Phys. Chem. C*, 2013, **117**, 7796.
34 E. Coutino-Gonzalez, D. Grandjean, M. B. J. Roeffaers, K. Kvashnina, B. Dieu, E. Fron, G. De Cremer, P. Lievens, B. Sels and J. Hofkens, *Chem. Commun.*, 2014, **50**, 1350.
35 E. Coutino-Gonzalez, M. B. J. Roeffaers, B. Dieu, G. De Cremer, S. Leyre, P. Hanselaer, W. Fyen, B. Sels and J. Hofkens, *J. Phys. Chem. C*, 2013, **117**, 6998.
36 E. Coutino-Gonzalez, W. Baekelant, D. Grandjean, M. B. J. Roeffaers, E. Fron, M. S. Aghakhani, N. Bovet, M. Van der Auweraer, P. Lievens, T. Vosch, B. Sels and J. Hofkens, *J. Mater. Chem. C*, 2015, **3**, 11857.
37 P. A. Jacobs, J. B. Uytterhoeven and K. H. J. Beyer, *J. Chem. Soc., Faraday Trans. 1*, 1979, **75**, 56.
38 S. Y. Kim, Y. Kim and K. Seff, *J. Phys. Chem. B*, 2003, **107**, 6938.
39 R. A. Schoonheydt and H. Leeman, *J. Phys. Chem.*, 1989, **93**, 2048.
40 M. D. Baker, G. A. Ozin and J. Godber, *J. Phys. Chem.*, 1985, **89**, 305.
41 B. Xu and L. Kevan, *J. Phys. Chem.*, 1992, **96**, 3647.
42 J. Texter, R. Kellerman and T. Gonsiorowski, *J. Phys. Chem.*, 1986, **90**, 2118.
43 E. Gachard, J. Belloni and M. A. Subramanian, *J. Mater. Chem.*, 1996, **6**, 867.
44 W. S. Ju, M. Matsuoka, K. Iino, H. Yamashita and M. Anpo, *J. Phys. Chem. B*, 2004, **108**, 2128.
45 S. M. Kanan, M. C. Kanan and H. H. Patterson, *J. Phys. Chem. B*, 2001, **105**, 7508.
46 K. Sawabe, T. Hiro, K. Shimizu and A. Satsuma, *Catal. Today*, 2010, **153**, 90.
47 T. Baba, H. Sawada, T. Takahashi and M. Abe, *Appl. Catal., A*, 2002, **231**, 55.
48 H. Yoshida, T. Hamajima, Y. Kato, J. Shibata, A. Satsuma and T. Hattori, *Res. Chem. Intermed.*, 2003, **29**, 897.
49 G. De Cremer, E. Coutino-Gonzalez, M. B. Roeffaers, D. E. De Vos, J. Hofkens, T. Vosch and B. F. Sels, *ChemPhysChem*, 2010, **11**, 1627.
50 A. Royon, K. Bourhis, M. Bellec, G. Papon, B. Bousquet, Y. Deshayes, T. Cardinal and L. Canioni, *Adv. Mater.*, 2010, **22**, 5282.
51 G. De Cremer, E. Coutino-Gonzalez, M. B. J. Roeffaers, B. Moens, J. Ollevier, M. Van der Auweraer, R. Schoonheydt, P. A. Jacobs, F. C. De Schryver, J. Hofkens, D. E. De Vos, B. F. Sels and T. Vosch, *J. Am. Chem. Soc.*, 2009, **131**, 3049.
52 O. M. Bakr, V. Amendola, C. M. Aikens, W. Wenseleers, R. Li, L. Dal Negro, G. C. Schatz and F. Stellacci, *Angew. Chem., Int. Ed.*, 2009, **48**, 5921.
53 I. Dıez and R. H. A. Ras, *Nanoscale*, 2011, **3**, 1963.
54 A. Mayoral, T. Carey, P. A. Anderson, A. Lubk and I. Diaz, *Angew. Chem., Int. Ed.*, 2011, **50**, 11230.
55 N. T. Cuong, H. M. T. Nguyen and M. T. Nguyen, *Phys. Chem. Chem. Phys.*, 2013, **15**, 15404.
56 H. Lin, K. Imakita and M. Fujii, *Appl. Phys. Lett.*, 2014, **105**, 211903.
57 P. Hohenberg and W. Kohn, *Phys. Rev. B: Condens. Matter Mater. Phys.*, 1964, **136**, 864.
58 R. Bauernschmitt and R. Ahlrichs, *Chem. Phys. Lett.*, 1996, **256**, 454.
59 M. E. Casida, C. Jamorski, K. C. Casida and D. R. Salahub, *J. Chem. Phys.*, 1998, **108**, 4439.
60 R. E. Stratmann, G. E. Scuseria and M. J. Frisch, *J. Chem. Phys.*, 1998, **109**, 8218.
61 C. Van Caillie and R. D. Amos, *Chem. Phys. Lett.*, 1999, **308**, 249.
62 F. Furche and R. Ahlrichs, *J. Chem. Phys.*, 2002, **117**, 7433.
63 A. D. Becke, *J. Chem. Phys.*, 1993, **98**, 5648.
64 P. J. Hay and W. R. Wadt, *J. Chem. Phys.*, 1985, **82**, 270.
65 M. J. Frisch, *et al.*, *Gaussian 09, Revision A.02*, Gaussian, Inc., Wallingford CT, 2009.
66 G. Karlström, R. Lindh, P.-Å. Malmqvist, B. O. Roos, U. Ryde, V. Veryazov, P.-O. Widmark, M. Cossi, B. Schimmelpfennig, P. Neogrady and L. Seijo, *Comput. Mater. Sci.*, 2003, **28**, 222.
67 P. A. Anderson, *Molecular Sieves*, Springer, Berlin, 2002, vol. 3.
68 H. Häkkinen, M. Moseler and U. Landman, *Phys. Rev. Lett.*, 2002, **89**, 033401.
69 B. O. Roos, R. Lindh, P.-Å. Malmqvist, V. Veryazov and P.-O. Widmark, *J. Phys. Chem. A*, 2005, **109**, 6575.
70 T. Steiner, *Angew. Chem., Int. Ed.*, 2002, **41**, 48–76.

